ELSEVIER

International Journal of Mass Spectrometry 202 (2000) 261–271

International Journal of Mass Spectrometry

Formation, photodissociation, and structure studies of group 14(Si, Ge, Sn, and Pb)/P binary cluster ions

Jian-bo Liu, Xiao-peng Xing, Peng Liu, Zhen Gao*

State Key Laboratory of Molecular Reaction Dynamics, Institute of Chemistry, Chinese Academy of Sciences, Beijing 100080, People's Republic of China

Received 15 November 1999; accepted 5 May 2000

Abstract

Group 14(Si, Ge, Sn, and Pb)/P binary cluster ions have been produced by laser ablation, photodissociated by UV laser and detected with a tandem time-of-flight mass spectrometer. As expected on the double periodicities of group 14 elements, Si/P and Ge/P binary cluster ions, whereas Sn/P and Pb/P binary cluster ions, have similar compositions, respectively. The stabilities of these binary phosphide cluster ions depend on their electronic and geometric structures, and the influence of geometric structures on the stabilities is increasing from Si/P cluster ions to Pb/P cluster ions. "Magic numbers" are observed in two types of binary phosphide cluster ions. One type of magic numbered binary cluster ions is isoelectronic to Zintl polyatomic anions (e.g. Pb_5^{2-}) in condensed phases. These binary cluster ions are composed of group 14 metals mainly, containing only one or two phosphorus atoms. The structures and bonding scheme of these binary cluster ions can be predicted by using Wade's electron counting rule. Another type of magic numbered binary cluster ions is isoelectronic either to the neutral group 14 clusters or to the neutral phosphorus clusters, and thus may present similar structures as their neutral analogues. The possible structures and bonding of the magic numbered cluster ions are further investigated with density functional theory Becke-style 3 parameter using the Lee-Yang-Parr correlation functional calculations. (Int J Mass Spectrom 202 (2000) 261–271) © 2000 Elsevier Science B.V.

Keywords: Group 14/phosphorus cluster ions; Laser ablation; Time-of-flight mass spectrometer; Photodissociation; Density functional theory calculations

1. Introduction

Group 14 (C, Si, Ge, Sn, and Pb) is an interesting series of elements because the bonding changes from covalent to metallic in going from the lightest to the heaviest element. Carbon has a strong covalent character, silicon and germanium are of the semiconductor type, whereas tin and lead are typical metals. This systematic variation in properties through the group is also presented in the gas phase clusters composed of group 14 elements. Carbon clusters C_n of a small size ($n < 10$) have chain structures, and the stabilities of cluster ions C_n^+ are dominated by the electronic structures and spin states [1–3]. Silicon clusters Si_n and germanium clusters Ge_n have similar compositions and structures but differ substantially from small carbon clusters [4–8]. Cyclic or closed structures are clearly more favorable for silicon clusters and germanium clusters over linear structures and there exist

* Corresponding author. E-mail: gaoz@mrdlab.icas.ac.cn

PII S1387-3806(00)00254-2

local maximum intensities (magic numbers) at $n = 6$, 10 for neutral Si_n, Ge_n and cations Si_n^+, Ge_n^+ [5]. Such similarities between silicon clusters and germanium clusters arise from the similarities in the valence wave functions of silicon and germanium. This effect is well known as "d-block screening", and a parallel effect leads to similarities between tin clusters Sn_n and lead clusters Pb_n. Both Sn_n and Pb_n have close packing geometries and the magic numbers $n = 7$, 10 [9,10].

From the comparison of these clusters, we can see obviously that the dominance of geometric structures on stabilities of group 14 clusters is gradually increased from the top element (C) to the bottom element (Pb), i.e. the close packing structures become more favorable when covalent bonding interaction is weakened. These trends could be attributed to many factors, such as valence electrons, ionization energies, electron affinities, atom sizes, etc., whereas the most profound factor is their bonding properties. However, since there is not enough experimental structure data available for gas phase group 14 clusters, it is still difficult to draw a general pattern governing their structures and stabilities in the gas phase.

In contrast to the gas phase group 14 cluster ions, the condensed phase group 14 cluster ions, particularly the condensed phase group 14 metal (also called post-transition metal) cluster ions, have been studied for many years. The most interesting result from condensed phase studies is that group 14 metals can form polyatomic Zintl ions, such as Ge_9^{2-}, Sn_5^{2-}, and Pb_5^{2-} [11], in which the bonding and structures can be followed by a simple electron counting scheme outlined in the form of Wade's rule [12–14]. In brief, for a polyhedron with N atoms, enhanced stability is expected for species containing $2N + 2$, $2N + 4$, and $2N + 6$ skeleton electrons. These electron counts define closo-(closed), nido-(nest-like) and arachno-(cobweb) cluster structures and determine the expected patterns in cluster bonding [15]. Zintl ions are normally produced in condensed phases, but it is now recognized that Zintl ions can also be produced in gas phase. It has been shown, for example, that the bonding in gas phase binary cluster ions $Cs_3Sn_5^+$, $Sn_2Bi_3^+$, and $Pb_2Bi_3^+$ are all related through this simple electron counting patterns [16–18]. The cesium atoms in $Cs_3Sn_5^+$ act as electron donors to match the electronic structure of Sn_5^{2-}. The tin, lead, and bismuth atoms in $Sn_2Bi_3^+$ or in $Pb_2Bi_3^+$ all participate in the construction of the closo skeletons to form ions isoelectronic to Sn_5^{2-} or Pb_5^{2-}. Martin has reported that binary clusters containing five lead atoms and a less electronegative element have a tendency to cluster into Pb_5^{2-} polyanions [15], which may also be explained by Wade's rule.

In this article gas phase binary cluster ions composed of group 14 element (Si, Ge, Sn, and Pb) and phosphorus are studied. The purpose of this investigation is to provide more insight into the role of the periodicity on group 14 clusters. Phosphorus can combine with every element of group 14 to form various phosphide compounds [18]. Liu et al. have reported the study of C/P binary cluster anions with the compositions of $C_nP_m^-$ [19]. In each composition the number of carbon atoms is much larger than that of phosphorus atoms, and the main compositions can be indicated as C_nP^- and $C_nP_2^-$. For the species C_nP^-, there is an odd/even oscillation in intensity, and the intensities with odd n are more intense than those with even n. Fisher et al. have performed density functional theory (DFT) calculations on the structures of C_nP^- and $C_nP_2^-$, and have shown that C_nP^- and $C_nP_2^-$ have optimized linear structures with P at one end of C_nP^- or two ends of $C_nP_2^-$, respectively [20]. From the present studies of Si, Ge, Sn, and Pb/P binary cluster ions, we expect to complete a systematical investigation of group 14 phosphide binary cluster ions, including the cluster compositions, electronic bonding, and geometric structures. From such studies we hope to understand the clustering properties of group 14 elements from another viewpoint.

Moreover, we also expect to examine the applicability of Wade's rule for these gas phase binary systems. Pure clusters of germanium, tin and lead since they contribute two p electrons for bonding per atom [14], are electron deficient. Their total valence electrons $2 \times N$ (N = atom number) is less than

$2N + 2$, $2N + 4$, . . . , and they exist as multicharged Zintl anions as Ge_9^{2-}, Sn_5^{2-}, and Pb_9^{4-} in condensed phases. A phosphorus atom, on the other hand, contributes three *p* electrons per atom and thus is electron rich. These trends average out in the group 14 phosphide cluster ions and thus precise electron counts ($2N + 2$, $2N + 4$, and $2N + 6$) can be achieved for single charged binary cluster ions in the gas phase. These binary clusters, therefore, provide another interesting test for Wade's rule in the gas phase because only certain stoichiometries can achieve desirable electron counts. Preferential combinations of elements according to Wade's electron counting rule, therefore, should appear as "magic numbered" peaks in the laser ablation time-of-flight (TOF) mass spectra.

2. Experiment and calculation

2.1. Experiment

The mixed samples were prepared by grinding the mixture of group 14 element (purity 99%) and red phosphorus (purity 99%) into fine powders, and pressing it into a tablet of 12 mm in diameter and 5 mm in thickness to form the laser target. The molar ratio for group 14 element to phosphorus in the mixed samples was varied from 1:1 to 1:8. Red phosphorus powder was pretreated to eliminate oxide impurities and kept dry in a phosphoric anhydride desiccator.

Experiments were performed on a homemade tandem time-of-flight mass spectrometer (TOFMS), the details of which were published elsewhere [21]. In brief, the sample target was mounted in the source chamber of the tandem TOFMS, which was evacuated to 10^{-4} Pa before laser ablation. The laser ablation was carried out by the second harmonic of a pulsed Nd:YAG laser (532 nm wavelength, 10 ns pulse width, 10 Hz, 10–20 mJ/pulse). The laser beam was focused with a lens ($f = 50$ cm) to a spot of diameter 0.5 mm on the target with the power density in order of 10^7 W/cm^2. The target surface under ablation was vaporized into a plume of plasma state consisting of electrons, ions, atoms, and cluster species formed from the ablation process and ion molecule reaction [22]. The cluster ions were extracted and accelerated by a pulsed voltage of 1.2 kV and then allowed to drift in a field-free region. After transmission through 3.5 m long field-free flight tube, the cluster ions with different masses were separated and detected by a dual microchannel plate detector. The mass resolution of the first stage of the tandem TOFMS is about 300. The cluster cations with a specific mass were selected by a mass gate at the end of the flight tube. The selected ions were decelerated by a retarding field of 0.9 kV and then photodissociated by an excimer laser beam (Lambda Physik LPX 300, KrF, 248 nm wavelength, 4 ns pulse width, 10 Hz, 200 mJ/cm^2). Following photodissociation, both the remaining parent ions and the fragment ions were reaccelerated and then mass analyzed by the second stage of the tandem TOFMS, which was perpendicular to the first stage. The signals from either the first stage or the second stage were recorded with a 10 MHz transient recorder, preamplified and stored in a PC computer. The final digitized mass spectrum was time averaged for over 2000 shoots.

2.2. Density function theory (DFT) calculation

Full geometry optimization was performed on selected binary cluster ions at several initial geometries, using the density functional method B3LYP (Becke-style 3-parameter using the Lee-Yang-Parr correlation functional) [23]. Vibrational analysis was performed on the optimized structures until a minimum with no imaginary vibrational frequencies was located. The basis set LANL2DZ was used for group 14 elements. This basis set treats the electrons near the nucleus in an approximate way by means of an effective core potential and also includes some relativistic effects, which are important for group 14 metal atoms [24]. For phosphorus, the basis set 6-31G(*d*) was used. All calculations were carried out by running GAUSSIAN 94 [25].

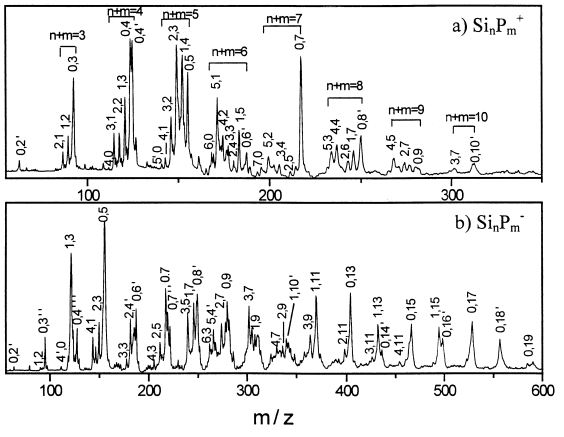

Fig. 1. TOF mass spectra of Si/P cluster ions produced by laser ablation of mixed samples of silicon and red phosphorus powder with Si:P = 1:1.

3. Results and discussion

3.1. Formation of group 14/P binary cluster ions

3.1.1. Si/P and Ge/P binary cluster ions

The mass spectra showing the positive and negative Si/P cluster ions produced by laser ablation are presented in Fig. 1(a) and (b). Although silicon and phosphorus have similar chemical properties, all possible compositions of binary cluster cations appear in the mass spectrum [Fig. 1(a)], which include $Si_nP_m^+$ as well as Si_n^+ and P_m^+. The peaks containing the same sum of atom numbers ($n + m$) are grouped in the mass spectrum. It is shown that for $n + m \leq 7$, the values of n and m vary continuously to form various cations $Si_nP_m^+$. For example, in case of $n + m = 4$, cations Si_4^+, Si_3P^+, $Si_2P_2^+$, SiP_3^+, and P_4^+ are all observed in the mass spectrum. However, for $8 \leq n + m \leq 10$, the number of phosphorus atoms in the binary cluster cations is larger than that of silicon atoms. These distributions are independent of the molar ration of Si/P in the mixed targets, indicating that they characterize the clustering ability of silicon and phosphorus. The experimental result also indicates that the self-clustering ability of phosphorus is stronger than that of silicon. This is consistent with the fact that P_m^+ of size m up to over 20 can be generated by laser ablation while Si_n^+ can only be produced to $n = 10$ under the same experimental condition.

The distribution of Si/P cluster anions is similar to that reported by Liu et al. before [19], which contains $Si_nP_m^-$, Si_n^-, and P_m^- [Fig. 1(b)]. The size of Si/P cluster anions is larger than that of Si/P cluster cations. Furthermore, the intensities of $Si_nP_m^-$ are oscillating with the number of phosphorus atoms, and the intensities of cluster anions with odd m are much more intense than those of the neighboring even m's. For example, $Si_nP_m^-$ with $n + m = 5$, intense peaks are corresponding to Si_4P^-, $Si_2P_3^-$, and P_5^-, whereas the peaks of $Si_3P_2^-$ and Si_4P^- are either much lower or absent in the mass spectrum. The odd/even oscillation of the intensity appears to correlate with the number of valence electrons in clusters. The valence electron number of the silicon atom is 2, and thus the number of clustered silicon atoms does not affect the parity of the cluster electron number. But the valence electron number of the phosphorus atom is 3. Therefore, the binary cluster anions with odd phosphorus atoms have all valence electrons paired (considering one additional electron for anions) and have no dangling bonds.

The experiment shows that most of bare $Si_n^\pm$ and bare $P_m^\pm$ with even m are hydrogenated with one hydrogen atom (the hydrogen atoms may come from trace impurities in red phosphorus), such as HSi_5^+, HP_2^+, HP_4^+, and HP_6^+ in cations and HSi_4^-, HP_6^-, and HP_8^- in anions. In particular, P_4^- is hydrogenated with three hydrogen atoms to form $H_3P_4^-$. However, for bare $P_m^\pm$ with odd m, there are intense signals observed for the bare clusters (i.e. not hydrogenated) or clusters hydrogenated only with even number of hydrogen atoms, such as $H_2P_3^-$. In Fig. 1(a) and (b), we use a prime to indicate hydrogen atoms in cluster ions, i.e. (0,2′) in Fig. 1(a) corresponds to HP_2^+, and (0,3″) in Fig. 1(b) corresponds to $H_2P_3^-$. This phenomenon again supports the idea that Si/P cluster ions prefer the even number electron system where all electrons can be paired up.

Fig. 1(b) reveals some intense peaks assigned to P_{5+4n}^- (n = 0–3), SiP_{3+4n}^- (n = 0–3), $Si_2P_{3+4n}^-$ (n = 0–2), $Si_3P_{3+4n}^-$ (n = 0–2), and $Si_3P_{5+4n}^-$

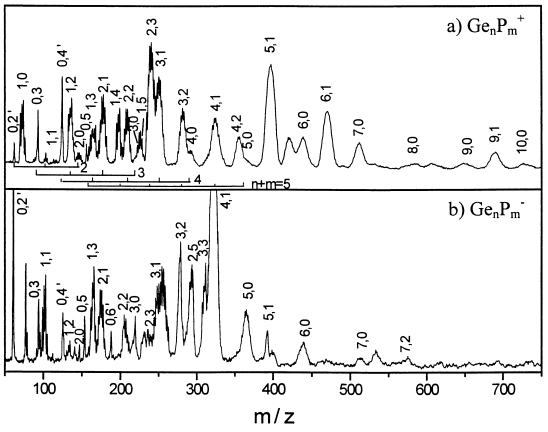

Fig. 2. TOF mass spectra of Ge/P cluster ions produced by laser ablation of mixed samples of germanium and red phosphorus powders with Ge:P = 1:4.

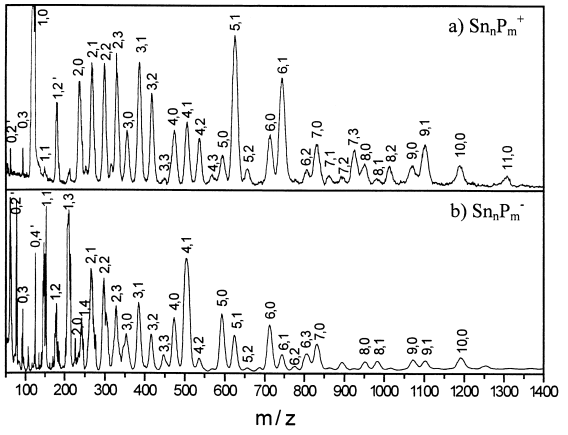

Fig. 3. TOF mass spectra of Sn/P cluster ions produced by laser ablation of mixed samples of tin and red phosphorus powders with Sn:P = 1:8.

($n = 0$–1). We note that these cluster anions all have paired valence electrons and their intensities are less affected by the molar ratio of Si/P in the targets, indicating they are thermodynamically stable. The fact that these anions grow by P_4 unit implies the possibility of attaching P_4 unit to the cluster skeletons during formation. Among these cluster anions, P_5^- has plane ring structure (D_{5h}) and compares to an aromatic 6π system [26]. SiP_3^- is isoelectronic to P_4 and should have a structure of tetrahedron [27]. SiP_7^- is isoelectronic to P_8 and may have a structure consisting of two tetrahedrons as P_8 [28]. In addition, we observed some cations isoelectronic to these cluster anions, i.e. P_5^+ and $Si_2P_3^-$, P_7^+ and $Si_2P_5^-$, SiP_5^+ and $Si_3P_3^-$, and SiP_7^+ and $Si_3P_5^-$. These analogues all have intense peaks in the mass spectra. Thus, it can be inferred that isoelectronic cluster species have similar stabilities. On the other hand, some positive and negative cluster ions with same isostoichimometries differ greatly in stabilities. It is conceivable, therefore, that the electron structure plays a more important role in determining the stability of Si/P cluster ions.

Due to the similarities in the chemical properties of silicon and germanium, the mass spectra of Ge/P binary cluster ions are expected to be similar with those of Si/P binary cluster ions. The fact that this is the case can be seen in Fig. 2(a) and (b). For $n + m \leq 5$, $Ge_nP_m^{\pm}$ have composition distributions similar to $Si_nP_m^{\pm}$ and contain all possible binary clusters with every n and m. However, for $n + m \geq 6$, the number of germanium atoms in binary cluster ions is larger than that of phosphorus atoms. Thus, the atom-clustering ability of germanium is a bit more intense than that of phosphorus. We note here that Ge/P binary cluster ions have magic numbers that are 2/3, 5/1, 6/1, and 9/1 for cations, and 1/3 and 4/1 for anions, which will be discussed in detail later.

3.1.2. Sn/P and Pb/P binary cluster ions

The mass spectra of Sn/P and Pb/P binary cluster ions are depicted in Figs. 3 and 4, which are very similar to each other. As shown in mass spectra, $Sn_nP_m^{\pm}$ and $Pb_nP_m^{\pm}$ can be divided into several groups according to the number of metal atoms contained in the clusters, and each group includes species with the same number of metal atoms and various numbers of phosphorus atoms. For the group of SnP_m^+ (or PbP_m^+), $SnHP_2^+$ (or $PbHP_4^+$) rather than SnP_2^+ (or PbP_4^+) is produced because the presence of a hydrogen atom helps the cluster to meet the condition of paired valence electrons in the cation. For the clusters of $Sn_2P_m^+$ and $Pb_2P_m^{\pm}$, only when m is odd, are the valence electrons in the cluster ions paired. So mass peaks of cluster ion with odd m are generally more intense than those with even m. When the size of clusters increases, the number of phosphorus atoms in

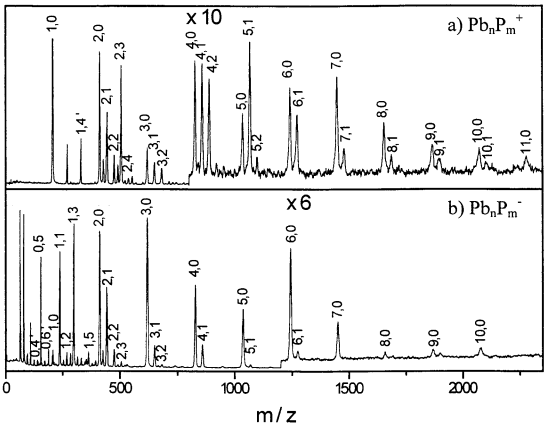

Fig. 4. TOF mass spectra of Pb/P cluster ions produced by laser ablation of mixed samples of lead and red phosphorus powders with Pb:P = 1:8.

clusters $Sn_nP_m^{\pm}$ and $Pb_nP_m^{\pm}$ decreases greatly. For example, $n \geq 10$ the cluster ions only exist as $Sn_n^{\pm}$ and $Pb_n^{\pm}$. Such distribution is not influenced by the composition of the targets but appear to be the intrinsic attributes of the binary clusters.

We also observed some magic numbers for Sn/P and Pb/P cluster ions, which are 2/3 (M = Sn, Pb), 5/1 (M = Sn, Pb), 6/1 (M = Sn, Pb), and 9/1 (M = Sn) for cations, and 1/3 (M = Sn, Pb) and 4/1 (M = Sn) for anions.

3.2. Photodissociation of group 14/P binary cluster cations

The photodissociation of cluster cations $Ge_nP_m^+$, $Sn_nP_m^+$, and $Pb_nP_m^+$ was carried out with a 248 nm excimer laser. Fig. 5 is typical mass spectra obtained from the photodissociation of Ge_5P^+, Sn_5P^+, and Pb_5P^+, respectively. As shown, there exist several photodissociation channels leading to M_4P^+, M_3P^+, M_2P^+ (M = Ge, Sn, Pb), etc. From the relative intensities of the fragment ions, we can estimate the efficiency R_i% of each photodissociation channel according to

$$R_i = \left(I_i \Big/ \sum_j I_j \right) \times 100\% \quad (1)$$

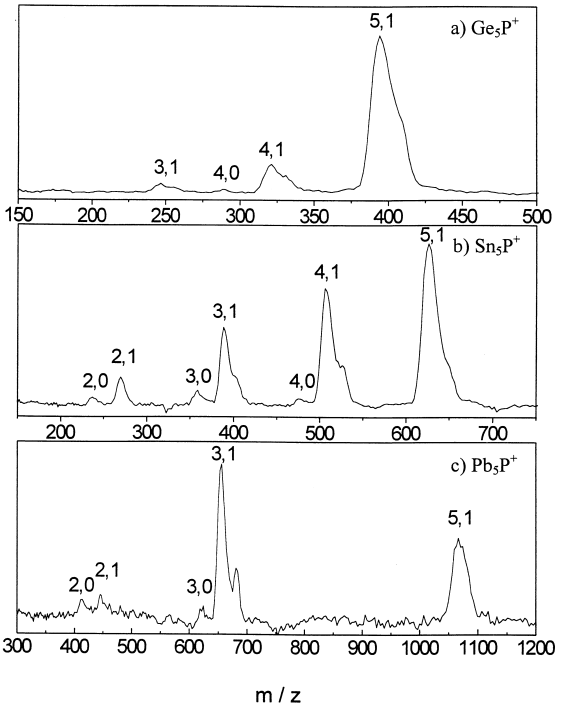

Fig. 5. Second-stage TOF mass spectra of the fragment ions of Ge_5P^+, Sn_5P^+ and Pb_5P^+ when photodissociated with the 248 nm laser.

where I_i is the intensity of the studied fragment ions and $\sum_j I_j$ is the intensities of all fragment ions including the remaining parent ions. We note that the photodissociation behavior of cluster cations is less sensitive to the power density of the photodissociation laser in the range of 200–400 mJ/cm^2. Table 1 summarizes the photodissociation channels and the corresponding efficiencies for each cation obtained with laser power of 400 mJ/cm^2.

It can be seen that Ge/P, Sn/P, and Pb/P binary cluster cations have a similar pattern of photodissociation, which implies similarities in their structures. For small cluster cations M_2P^+ the main photodissociation channel is the detachment of neutral phosphorus atom, indicating that the metal/metal bond is stronger than metal/phosphorus bond. For the same reason $M_2P_3^+$ has the main photodissociation channel of $M_2P^+ + P_2$. However, the main photodissociation channels of the larger cluster cations ($n > 3$) are

Table 1
Photodissociation channels and photodissociation efficiencies of group 14/P binary cluster cations

Parent ion	Channel	R_i%	Parent ion	Channel	R_i%	Parent ion	Channel	R_i%
Ge_2P^+	$Ge_2^+ + P$	4	Sn_2P^+	$Sn_2^+ + P$	9	Pb_2P^+	$Pb_2^+ + P$	8
	$GeP^+ + Ge$	2					$PbP^+ + Pb$	5
	$Ge_2^+ + GeP$	2					$Pb^+ + PbP$	7
$Ge_2P_3^+$	$Ge^2P^+ + P_2$	13	$Sn_2P_3^+$	$Sn_2P^+ + P_2$	9	$Pb_2P_3^+$	$Pb_2P^+ + P_2$	3
							$PbP_2^+ + PbP$	10
Ge_3P^+	$Ge_3^+ + P$	1	Sn_3P^+	$Sn_3^+ + P$	2	Pb_3P^+	$Pb_3^+ + P$	3
	$Ge_2P^+ + Ge$	9		$Sn_2P^+ + Sn$	19		$Pb_2P^+ + Pb$	3
	$Ge_2^+ + GeP$	2		$Sn_2^+ + SnP$	7		$Pb_2^+ + PbP$	14
	$Ge^+ + Ge_2P$	1		$Sn^+ + Sn_2P$	2		$Pb^+ + Pb_2P$	3
$Ge_3P_2^+$	$Ge_3P^+ + P$	1	$Sn_3P_2^+$	$Sn_3P^+ + P$	3	$Pb_3P_2^+$		
	$Ge_3^+ + P_2$	4		$Sn_3^+ + P_2$	7			
	$Ge_2P^+ + GeP$	1						
	$Ge_2^+ + GeP_2$	1					$Pb_2^+ + PbP_2$	42
Ge_4P^+	$Ge_3P^+ + Ge$	10	Sn_4P^+	$Sn_3P^+ + Sn$	25	Pb_4P^+		
				$Sn_3^+ + SnP$	2		$Pb_3^+ + PbP$	9
	$Ge_2P^+ + Ge_2$	2		$Sn_2P^+ + Sn_2$	12		$Pb_2P^+ + Pb_2$	18
	$Ge_2^+ + Ge_2P$	1		$Sn_2^+ + Sn_2P$	4		$Pb_2^+ + Pb_2P$	3
Ge_5P^+	$Ge_4P^+ + Ge$	12	Sn_5P^+	$Sn_4P^+ + Sn$	28	Pb_5P^+		
	$Ge_3P^+ + Ge_2$	5		$Sn_3P^+ + Sn_2$	15		$Pb_3P^+ + Pb_2$	66
				$Sn_2P^+ + Sn_3$	6		$Pb_2P^+ + Pb_3$	2
Ge_6P^+	$Ge_5P^+ + Ge$	15	Sn_6P^+	$Sn_5P^+ + Sn$	27			
				$Sn_4P^+ + Sn_2$	5			
	$Ge_4^+ + Ge_2P$	2		$Sn_4^+ + Sn_2P$	2			
				$Sn_3P^+ + Sn_3$	6			

different from those of small cluster cations, i.e. the metal atoms rather than the phosphorus atoms are stripped from the clusters in the photodissociation process. The cations M_4P^+, M_5P^+, and M_6P^+ have the dissociation channels of $M_3P^+ + M$, $M_4P^+ + M$, and $M_5P^+ + M$, respectively, where one metal atom is stripped. The fragment cations M_3P^+, M_4P^+, and M_5P^+ are also found as intensive peaks in the laser ablation mass spectra, which indicates that these fragments have stable structures.

3.3. Structures and bonding of magic numbered group 14/P binary cluster ions

As shown from above discussion, cluster magic numbers of 2/3 ($M_2P_3^+$, M = Ge, Sn, Pb), 5/1 (M = Ge, Sn, Pb), 6/1 (M = Ge, Sn, Pb), and 9/1 (M = Ge, Sn) are observed for the binary cluster cations, and 1/3 (M = Ge, Sn, Pb) and 4/1 (M = Ge, Sn) for the binary cluster anions. These magic numbers indicate the particular stable electronic and/or geometric structures. Here, the possible structures of these magic numbers are predicted based on Wade's rule and further confirmed by B3LYP calculations using the LANL2DZ basis set for metals and 6-31G(*d*) basis set for P. Structures, which are local minima on potential surface from B3LYP calculations, are characterized rigorously by the presence of all positive eigenvalues of the force constant matrix, i.e. no imaginary frequencies.

3.3.1. Binary cluster cations 5/1 and 9/1

The binary cluster cations M_5P^+ and M_9P^+ have valence electrons 12 and 20, respectively (each group 14 metal atom contributes two *p* electrons and phosphorus atom contributes three *p* electrons). If a phosphorus atom attaches itself as an electron-donating ligand to the cluster skeletons, then M_5P^+ and M_9P^+ are, respectively, isoelectronic to M_5^{2-} and M_9^{2-} Zintl anions.

By Wade's rule, M_5^{2-} has a structure of trigonal bipyrimid, and thus M_5P^+ may have a similar trigonal

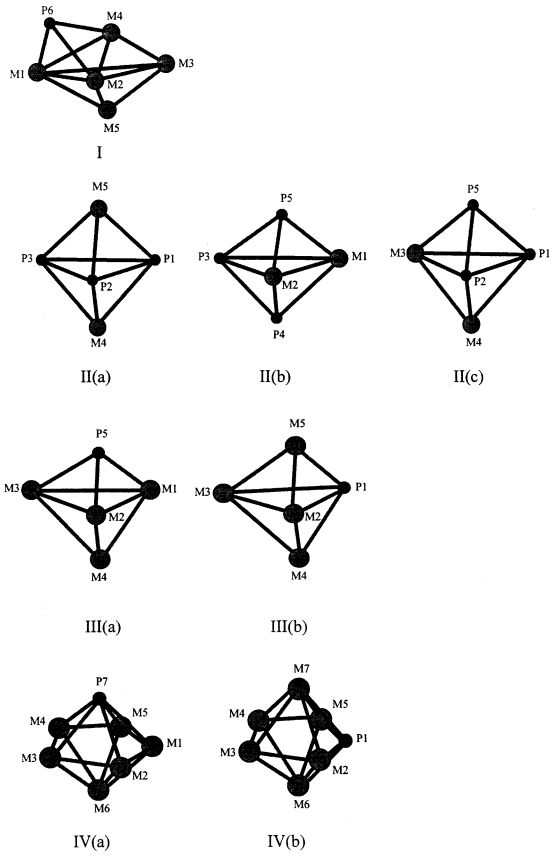

Fig. 6. Proposed structures of I, M_5P^+; II(a), II(b), and II(c), $M_2P_3^+$; III(a) and III(b) M_4P^-; IV(a) and IV(b), M_6P^+.

bipyrimid skeleton attached by a phosphorous atom additionally. In order to confirm this prediction, the possible structures of Ge_5P^+ and Sn_5P^+ were studied with B3LYP calculations. The optimized structures of Ge_5P^+ and Sn_5P^+ are shown as (I) in Fig. 6. The calculation results are listed in Table 2. In structure (I), five metal atoms construct trigonal bipyrimid skeleton, and three metal atoms M1, M2, and M4 are connected to a phosphorus atom. With this configuration M3 and M5 are relatively bonded weakly compared with the remaining three metal atoms and thus are easily stripped on photodissociation, which is consistent with the photodissociation results. As noted already, for M_5P^+ the most efficient fragmentation is the neutral loss of one or two metal atoms.

The bonding scheme in M_5P^+ can be rationalized in terms of multicenter bonds. Each metal atom contributes three *p* orbitals and two *p* valence electrons to the cluster skeleton, and each phosphorus atom contributes three *p* orbitals and three *p* valence electrons, thus total eighteen *p* orbitals and twelve *p* electrons are included in the M_5P^+ skeleton. Supposing that M_5P^+ is constructed by "*d*" pairs of two-center two-electron M–M bonds and "*t*" pairs of three-center two-electron M–M–M bonds, and a phosphorus atom is connected to the skeleton by three pairs of two-center two-electron M–P bonds, then we

Table 2
Optimized geometries for M_5P^+ (M = Ge, Sn) obtained by B3LYP/LANL2DZ for M, 6-31G(*d*) for P

Cluster	Atomic distance (Å)							Atomic charge
Ge_5P^+	Ge2–Ge1	3.232	Ge3–Ge2	4.398	Ge5–Ge3	2.455	Ge1	0.370
	Ge3–Ge1	4.398	Ge4–Ge2	3.258	P6–Ge3	4.853	Ge2	0.370
	Ge4–Ge1	3.258	Ge5–Ge2	2.655	Ge5–Ge4	2.970	Ge3	0.378
	Ge5–Ge1	2.655	P6–Ge2	2.437	P6–Ge4	2.475	Ge4	0.206
	P6–Ge1	2.437	Ge4–Ge3	2.835	P6–Ge5	3.593	Ge5	−0.103
							P6	−0.221
Sn_5P^+	Sn2–Sn1	3.590	Sn3–Sn2	4.997	Sn5–Sn3	2.793	Sn1	0.456
	Sn3–Sn1	4.996	Sn4–Sn2	3.615	P6–Sn3	5.342	Sn2	0.456
	Sn4–Sn1	3.615	Sn5–Sn2	3.032	Sn5–Sn4	3.345	Sn3	0.378
	Sn5–Sn1	3.032	P6–Sn2	2.598	P6–Sn4	2.650	Sn4	0.286
	P6–Sn1	2.598	Sn4–Sn3	3.210	P6–Sn5	3.922	Sn5	−0.107
							P6	−0.469

have $d = -3$ and $t = 6$. This result is, of course, impossible. Alternatively, if M_5P^+ is constructed by d pairs of two-center two-electron M–M and M–P bonds, and t pairs of three-center two-electron M–M–M and M–P–M bonds (i.e. phosphorus is involved in multicenter bonding), then we have $d = 0$ and $t = 6$. It means that M_5P^+ is constructed by multicenter bonds exclusively, which includes three pairs of M–M–M bonds and three pairs of M–P–M bonds. In this picture, stable polyhedral clusters are formed when multicenter bonds delocalize throughout the cluster and achieve various resonant configurations. This delocalized picture of cluster bonding in three dimensions is analogous to aromaicity in two dimension structures (e.g. benzene).

Likewise, the structure and bonding of M_9P^+ can be predicted by Wade's rule. Nine metal atoms in M_9P^+ build up a tricapped trigonal prism polyhedron as Ge_9^{2-} [11,12], to which a phosphorus atom as an electron donor is attached.

3.3.2. Binary cluster cations 2/3 and anions 4/1

The stabilities of cations $M_2P_3^+$ and anions M_4P^- can be expected by the Wade's rule, too. However, unlike M_5P^+ and M_9P^+, in $M_2P_3^+$ and M_4P^- the phosphorus atoms join directly to the polyhedral skeletons rather than attach to the skeletons as ligands. Wade's rule is satisfied for $M_2P_3^+$ and M_4P^- as 12(electrons) = $2N$(atoms) + 2, and their structures should be trigonal bipyrimid by Wade's rule. In both $M_2P_3^+$ and M_4P^-, there should be three pairs of two-center two-electron bonds and three pairs of three-center two-electron bonds.

There are three possible trigonal bipyrimid structures of $M_2P_3^+$ shown as II(a), II(b), and II(c) in Fig. 6, corresponding to D_{3h}, C_{2v}, and C_s symmetry respectively. In structure II(a), both two phosphorus atoms are located at the vertices of the trigonal bipyramid, while in structure II(b) and II(c), either one or two phosphorus atoms are located on the plane of the trigonal bipyrimid. The B3LYP calculations for $Ge_2P_3^+$ and $Sn_2P_3^+$ give the stability sequence as II(a) > II(c) > II(b), the structure II(a) with the highest symmetry is the most stable one. The energy difference between these structural isomers is listed in Table 3.

For Ge_4P^- and Sn_4P^-, B3LYP calculations have been done on two possible structures III(a) and III(b), shown in Fig. 6. Since III(a) and III(b) are similar and can convert to each other, the energy difference between III(a) and III(b) is quite small. The structure III(a) with higher symmetry (C_{3v}) is a bit more stable than III(b) (C_{2v}) (see Table 3).

3.3.3. Binary cluster cations 6/1 and anions 1/3

The cation M_6P^+ and anion MP_3^- are, respectively, isoelectronic to neutral M_7 (M = Ge, Sn, Pb) and P_4. 7 is a magic number of neutral clusters of group 14 elements, which has a structure of pentagonal bipyrimid [4,9,29,30], while 4 is a magic number of the neutral phosphorus cluster which has a structure of tetrahedron [27]. M_6P^+ and MP_3^- may have structures of pentagonal bipyrimid like M_7 and tetrahedron like P_4, respectively. Based on these guesses, two possible pentagonal bipyrimid structures of Ge_6P^+ and Sn_6P^+, IV(a) (C_{5v}) and IV(b) (C_{2v}), have been calculated by B3LYP. In structure IV(a) the phosphorus atom is located at one vertex of the pentagonal bipyrimid, while in structure IV(b) it is located on the pentagonal plane. As expected, the energy of structure IV(a) with a higher symmetry is at a local minimum.

4. Conclusions

Both positive and negative group 14 (Si, Ge, Sn, Pb)/phosphorus binary cluster ions were produced by laser ablation. The composition and intensity distributions of these binary cluster ions vary with each different group 14 element. The Si/P binary cluster ions display the most abundant compositions. The formation process of $Si_nP_m^{\pm}$ can be viewed as substitution of phosphorus atoms by silicon atoms from pure $P_{n+m}^{\pm}$ where the numbers of n and m change continuously. The relative intensity of $Si_nP_m^{\pm}$ correlates with the relative stability of $P_{n+m}^{\pm}$. It is known that P_7^+ is the most stable among P_{n+m}^+ [28], then in the series of $Si_nP_m^{\pm}$ with $n + m = 7$, the signal of P_7^+ is the most intense one. For $Ge_nP_m^{\pm}$, $Sn_nP_m^{\pm}$, and $Pb_nP_m^{\pm}$, the binary cluster ions of small sizes ($n \leq 5$) are composed of metal atoms and phosphorus atoms

Table 3
Calculation results for different structures of $M_2P_3^+$, M_4P^-, and M_6P^+ (M = Ge, Sn) by B3LYP/LANAL2DZ for M, 6031G(*d*) for P

Cluster	Structure	ΔE (eV)	Atomic distance (Å)						Atomic charge	
$Ge_2P_3^+$	II(a)	0.0	P2–P1	2.301	P3–P2	2.301	Ge5–P3	2.493	P1	−0.056
			P3–P1	2.301	Ge4–P2	2.493	Ge5–P4	4.218	P2	−0.056
			Ge4–P1	2.493	Ge5–P2	2.493			P3	−0.056
			Ge5–P1	2.493	Ge4–P3	2.493			Ge4	0.584
									Ge5	0.584
	II(b)	0.616								
	II(c)	0.471								
$Sn_2P_3^+$	II(a)	0.0	P2–P1	2.301	P3–P2	2.301	Sn5–P3	2.669	P1	−0.163
			P3–P1	2.301	Sn4–P2	2.669	Sn5–P4	4.629	P2	−0.163
			Sn4–P1	2.669	Sn5–P2	2.669			P3	−0.163
			Sn5–P1	2.669	Sn4–P3	2.669			Sn4	0.745
									Sn5	0.745
	II(b)	0.866								
	II(c)	0.707								
Ge_4P^-	III(a)	0.0	Ge2–Ge1	2.956	Ge3–Ge2	2.956	P5–Ge3	2.442	Ge1	−0.112
			Ge3–Ge1	2.956	Ge4–Ge2	2.680	P5–Ge4	3.813	Ge2	−0.112
			Ge4–Ge1	2.680	P5–Ge2	2.442			Ge3	−0.112
			P5–Ge1	2.442	Ge4–Ge3	2.680			Ge4	−0.225
									P5	−0.439
	III(b)	0.027								
Sn_4P^-	III(a)	0	Sn2–Sn1	3.288	Sn3–Sn2	3.288	P5–Sn3	2.621	Sn1	−0.053
			Sn3–Sn1	3.288	Sn4–Sn2	3.042	P5–Sn4	4.185	Sn2	−0.053
			Sn4–Sn1	3.042	P5–Sn2	2.621			Sn3	−0.053
			P5–Sn1	2.621	Sn4–Sn3	3.042			Sn4	−0.245
									P5	−0.596
	III(b)	0.009								
Ge_6P^+	IV(a)	0	Ge2–Ge1	2.791	Ge4–Ge2	4.515	P7–Ge3	2.634	Ge1	0.318
			Ge3–Ge1	4.515	Ge5–Ge2	4.515	Ge5–Ge4	2.791	Ge2	0.317
			Ge4–Ge1	4.515	Ge6–Ge2	2.833	Ge6–Ge4	2.833	Ge3	0.318
			Ge5–Ge1	2.791	P7–Ge2	2.634	P7–Ge4	2.634	Ge4	0.317
			Ge6–Ge1	2.833	Ge4–Ge3	2.791	Ge6–Ge5	2.833	Ge5	0.318
			P7–Ge1	2.634	Ge5–Ge3	4.515	P7–Ge5	2.634	Ge6	−0.013
			Ge3–Ge2	2.791	Ge6–Ge3	2.833	P7–Ge6	2.689	P7	−0.575
	IV(b)	0.265								
Sn_6P^+	IV(a)	0	Sn2–Ge1	3.081	Sn4–Sn2	4.984	P7–Sn3	2.807	Sn1	0.355
			Sn3–Ge1	4.984	Sn5–Sn2	4.984	Sn5–Sn4	3.081	Sn2	0.356
			Sn4–Ge1	4.984	Sn6–Sn2	3.218	Sn6–Sn4	3.218	Sn3	0.355
			Sn5–Ge1	3.081	P7–Sn2	2.807	P7–Sn4	2.807	Sn4	0.356
			Sn6–Ge1	3.218	Sn4–Sn3	3.081	Sn6–Sn5	3.218	Sn5	0.355
			P7–Ge1	2.807	Sn5–Sn3	4.984	P7–Sn5	2.807	Sn6	0.045
			Sn3–Sn2	3.081	Sn6–Sn3	3.218	P7–Sn6	2.875	P7	−0.822
	IV(b)	0.470								

with nearly all possible compositions, while those of larger sizes ($n > 5$) mainly contain metal atoms. In summary, from silicon to lead the atomic clustering ability of group 14 elements increases and is preferred to binary clustering with phosphorus.

The stabilities of group 14/phosphorus cluster ions depend on both electronic and geometric structures. The cluster ions prefer to have all valence electrons paired up, and some clusters pick up hydrogen atoms to achieve this result. The close packing structures are much favored for these binary cluster ions, and most isoelectronic cluster species have similar structures and stabilities.

Zintl type binary cluster ions have been observed

for Ge/P, Sn/P, and Pb/P binary cluster ions. The bonding and structures for these cluster ions can be predicted by Wade's rule. This prediction, together with the results of DFT calculations, further confirms that isoelectronic clusters exhibit similar structures and stabilities. One feature observed in these clusters is that group 14 metals are still liable to form closo polyhedron in the gas phase as they are in condensed phases. These studies provide further connection between cluster studies in the gas and in condensed phases.

References

[1] W.L. Brown, R.R. Freeman, K. Raghavachari, M. Schluter, Science 235 (1987) 860.
[2] K.B. Shelimov, J.M. Hunter, M.F. Jarrold, Int. J. Mass Spectrom. Ion Processes 138 (1994) 17.
[3] G. von Helden, N.G. Gotts, W.E. Palke, M.T. Bowers, Int. J. Mass Spectrom. Ion Processes 138 (1994) 33.
[4] G. Pacchioni, J. Koutecký, J. Chem. Phys. 84 (1986) 3301.
[5] J.R. Heath, Y. Liu, S.C. O'Brein, Q.L. Zhang, R.F. Curl, F.K. Tittle, R.E. Smalley, J. Chem. Phys. 83 (1985) 5520.
[6] M.F. Jarrold, in Modern Inorganic Chemistry, D.H. Russell (Ed.), Plenum, New York, 1989.
[7] J.M. Hunter, J.L. Fye, M.F. Jarrold, J.E. Bower, Phys. Rev. Lett. 73 (1994) 2063.
[8] P. Jackson, K.J. Fisher, G.E. Gadd, I.G. Dance, D.R. Smith, G.D. Willett, Int. J. Mass Spectrom. Ion Processes 164 (1997) 45.
[9] P. Jackson, I.G. Dance, K.J. Fisher, G.D. Willett, G.E. Gadd, Int. J. Mass Spectrom. Ion Processes 157/158 (1996) 329.
[10] K. Laihing, R.G. Wheeler, W.L. Wilson, M.A. Duncan, J. Chem. Phys. 87 (1987) 3401.
[11] J.D. Corbett, Chem. Rev. 85 (1985) 383.
[12] K. Wade, Adv. Inorg. Chem. Radiochem. 18 (1976) 1.
[13] G. Gonzalez-Moraga, Cluster Chemistry, Springer, Berlin, 1993, p. 267.
[14] D. Michael, P. Migos, Chem. Soc. Rev. 15 (1986) 31.
[15] T.P. Martin, J. Chem. Phys. 83 (1985) 78.
[16] R.G. Wheeler, K. Laihing, W.L. Wilson, M.A. Duncan, J. Chem. Phys. 88 (1988) 2831.
[17] D. Schild, R. Pflaum, K. Sattler, E. Recknagel, J. Phys. Chem. 91 (1987) 2649.
[18] H.-G. von Schnering, W. Honle, Chem. Rev. 88 (1988) 243.
[19] Z.Y. Liu, R.B. Huang, L.S. Zheng, Z. Phys. D 38 (1996) 171.
[20] K. Fisher, I. Dance, G. Willett, Eur. Mass. Spectrom. 3 (1997) 331.
[21] Z. Gao, F.A. Kong, X.J. Wu, N. Zhang, Q.H. Zhu, Z.P. Zhang, Q.Z. Lu, Chin. J. Chem. Phys. 5 (1992) 343.
[22] M.L. Mandich, W.D. Reents, V.E. Bondyley, in Atomic and Molecular Clusters, E.R. Berstein (Ed.), Elsevier, Amsterdam, 1990, Chap. 2.
[23] A.D. Becke, J. Chem. Phys. 98 (1993) 5648.
[24] J.B. Foresman, A. Frisch, Exploring Chemistry with Electronic Structure Methods, Gaussian, Inc., Pittsburgh, PA, 1995.
[25] GAUSSIAN 94, revision E.1, M.J. Frisch, G.W. Trucks, H.B. Schlegel, P.M.W. Gill, B.G. Johnson, M.A. Robb, J.R. Cheeseman, T. Keith, G.A. Petersson, J.A. Montgomery, K. Raghavachari, M.A. Al-Laham, V.G. Zakrzewski, J.V. Ortiz, J.B. Foresman, J. Cioslowski, B.B. Stefanov, A. Nanayakkara, M. Challacombe, C.Y. Peng, P.Y. Ayala, W. Chen, M.W. Wong, J.L. Andres, E.S. Replogle, R. Gomperts, R.L. Martin, D.J. Fox, J.S. Binkley, D.J. Defrees, J. Baker, J.P. Stewart, M. Head-Gordon, C. Gonzalez, and J.A. Pople, Gaussian, Inc., Pittsburgh, PA, 1995.
[26] R.O. Jones, G. Ganteför, S. Hunsicker, P. Pieperhoff, J. Chem. Phys. 103 (1995) 9549.
[27] F.A. Cotton, G. Wilkinson, Advanced Inorganic Chemistry, Wiley, New York, 1988.
[28] R.B. Huang, H.D. Li, Z.Y. Lin, S.H. Tang, J. Phys. Chem. 99 (1995) 1418.
[29] J.C. Philips, Chem. Rev. 86 (1986) 619.
[30] K. Raghavachari, C.M. Rohlfing, J. Chem. Phys. 89 (1988) 2219.